Carbon-coated Cu nanoparticles as heterogeneous catalysts for cycloaddition of propargylamine to cyclic ketones

Dmytro V. Yehorov,[a,b] Svitlana O. Sotnik,[a,c] Vitalii M. Asaula,[c] Olena O. Pariiska,[c] Evgenia V. Senchylo,[c] Illia Pavliei,[a,c,d] Igor E. Kotenko,[c] Anastasiya V. Terebilenko,[c] Alexander B. Rozhenko,[b] Konstantin S. Gavrilenko,[a,d] Serhiy V. Ryabukhin,[a,b,d] Dmytro M. Volochnyuk,[a,b,d] Sergey V. Kolotilov[a,c,d]

[a]Enamine Ltd., *78 Winston Churchill Street, Kyiv, 02094, Ukraine*

[b]Institute of Organic Chemistry, National Academy of Sciences of Ukraine, *5 Akademik Kukhar Street, Kyiv, 02094, Ukraine*

[c]L.V. Pisarzhevskii Institute of Physical Chemistry, National Academy of Sciences of Ukraine, *31 Nauki Avenue, Kyiv, 03028, Ukraine*

[d]Taras National Shevchenko University of Kyiv, *60 Volodymyrska Street, Kyiv, 01033, Ukraine*

Abstract

A set of 22 composites was prepared by pyrolysis of Cu^{2+} complexes with phenanthroline and 1,2-diaminobenzene, deposited on SiO_2 (Aerosil). All composites contained Cu and carboneous components, while some of them additionally contained Cu_2O or CuCl. According to the data of powder X-ray diffraction, the size of Cu nanoparticles was 20-37 nm. The presence of Cu nanoparticles was confirmed by TEM, while some aggregates were found by SEM. The composites were tested as the heterogeneous catalysts in the process of cycloaddition of propargylamine with 4-oxocyclohexanecarboxylate leading to ethyl 5,6,7,8-tetrahydroquinoline-6-carboxylate. It was found that the product yield did not correlate with Cu content in the reaction mixture or other single parameters, but reached maximal values at certain values of parameters, proportional to the surface of Cu and surface of C, exposed to the reagents. It was found that the leaching of Cu takes place upon repeated use of the composites.

Key words: copper, pyrolysis, nanoparticles, catalyst, cycloaddition, fused pyridine

Cycloalkane ring-fused pyridines are valuable small hydrophilic sp^3-saturated building blocks for medicinal chemistry[1,2]. Such pyridines can be found in several biologically active molecules, such as antibiotics[3], antifungals[4], medicines for Alzheimer's disease treatment[5], as well as antitumor and anticancer drugs[6,7]. A series of CXCR4 antagonists bearing 5,6,7,8-tetrahydroquinoline fragment was reported [8–10]. Wide application is a reason for the significant importance of this building block. Hydrogenation of the pyridine ring in the cycloalkane ring-fused

pyridines leads to the respective cycloalkane-fused piperidines, which also hold a position among the most popular scaffolds in medicinal chemistry[11].

During the last century, the methods of cycloalkane ring-fused pyridines preparation evolved from multi-step sequences to single-step atom-efficient reactions mostly based on cyclic ketones as the starting materials. Several single-step methods of cycloalkane fused pyridines synthesis were reported. Abbiaty *et. al.* described a preparative method for the synthesis of cycloalkenopyridines from cyclic ketones and propargylamine[12]. In this seminal study, it was shown that sodium tetrachloroaurate was the most suitable and reliable catalyst for this reaction. Later, metallic nanoparticles (Au, Ag, Cu) deposited on alumina were used as catalysts for the oxidative cyclization of enamines, obtained from propargylamine and ketones[13]. Again, it was found that Au-containing systems had the best performance, while the use of Cu-impregnated alumina as a catalyst led to *ca*. 70 % conversion of ketone (such as acetone) to pyridine (such as 2-picoline) at 125 °C and 5 bar pressures of oxygen. However, the conversion of acetone fell to *ca*. 45 % after 1.5 h[13]. Recently we showed that Cu^{II} salts could be used as the catalysts for multigram synthesis of fused pyridines[14]. The use of air at ambient pressure instead of pressurized oxygen was an additional advantage of our method.

At the same time, the pharmaceutical industry requires compounds in kilograms or even larger scales, so development of the methods suitable for implementation in flow reactors is the logical continuation of the synthetic evolution. To achieve high performance, switching from homogeneous to heterogeneous catalysis seems to be almost inevitable. In addition, the use of heterogeneous catalysts leads to the simplification of product purification from the contamination of the metal ions, facilitates reuse, and reduces e-factor (i.e., a quantity of waste and pollution of the environment)[15–17].

Heterogenization of the metal-containing catalysts is accompanied by the problem of the active component dispersion because only surface can participate in reactions in the case of solids. High dispersion of the catalytically active sites can be achieved by their incorporation into the structure of porous material[18–20] or deposition of catalytically active species on the support with a high specific surface, the latter approach has been commonly used for development of the catalytically active composites[21–23]. Metal-organic frameworks or coordination polymers can contain accessible catalytically active metal ions in each structural motif, for example, Cu^{II} 1,2,3-benzenetricarboxylate can be an efficient catalyst with the highly accessible surface[14,24–26].

A combination of different metals and a porous matrix with known texture characteristics makes it possible to obtain composite materials with desired catalytic and sorption properties[27,28]. By varying the content and chemical properties of the porous material such as acidic and basic sites or redox centers, and the nature of the incorporated metal, a multifunctional catalyst suitable for tandem catalysis can be obtained[28]. Immobilization of the metallic particles on porous supports such

as porous organic polymers ([29,30]), covalent organic framework [31,32], metal-organic frameworks, zeolites[33,34], SiO_2 [35–37], TiO_2[38,39], CeO_2[40] and other porous materials is widely used for design of the catalyst for many processes. Such materials exhibit catalytic activity in the CO oxidation[16,36], CO_2 methanation[41], oxidation of benzylic C–H bond[29,30], hydrogenation of nitroaromatics[27,39,42], nitriles[37], reductive N-alkylation of amides[43], Ullmann reactions[38], Suzuki–Miyaura Coupling Reaction[31] and so on.

In this study, we intended to develop the heterogeneous Au-free catalyst of oxidative annulation of cyclic ketones with propargylamine, suitable for use in the flow reactors, and to find conditions for high yields of the fused pyridines in the presence of such systems in an atmosphere of air (as we managed in our previous study for $CuCl_2$[14]). The idea of the work was that Cu-containing composites, prepared by thermal decomposition of Cu^{II} complexes with DAB and Phen (where DAB is 1,2-diaminobenzene, Phen is 1,10-phenanthroline) on SiO_2 surface, would have high catalytic performance in the Cu-catalyzed process, similarly to the previously reported cases where catalytically active metal-containing composites were prepared by pyrolysis [44–48]. Thermal decomposition of Cu^{II} complexes was chosen as the method for preparation of the catalysts due to its simplicity and suitability for scale-up, which is important in the case of preparation of large batches of the catalysts. SiO_2 used was Aerosil, it was chosen as a solid porous support for the immobilization of Cu species because of its high surface, thermal stability as well as stability under the reaction conditions, and, in addition, its low price.

The composites obtained herein are marked as Cu@SiO_2-X, where X is the entry number (Table 1). A significant quantity of carbon was also found in the samples, and we supposed that the carboneous component could make influence on the catalytic performance of the samples[45,49] (it was previously supposed that the carboneous materials could have catalytic activity in organic reactions[50,51]]). The resulting composites were studied by XRD, SEM, TEM, RAMAN and EDX; the catalytic properties of the composites in the reaction of ethyl 4-oxocyclohexanecarboxylate with propargylamine leading to ethyl 5,6,7,8-tetrahydroquinoline-6-carboxylate (Scheme 1) were tested. This reaction was chosen as a model because of the simple spectral characterization of the reaction mixtures, the non-volatility of the starting ketone and the product, and the importance of the product as the starting compound for fine organic synthesis.

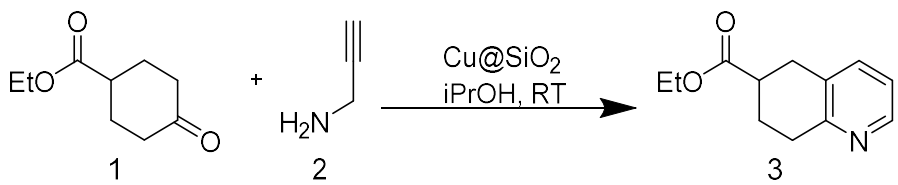

Figure 1. Reaction of ethyl cyclohexa-4-one-1-carboxylate with propargylamine catalyzed be Cu@SiO_2

Experimental

Commercially available reagents – copper(II) acetate hydrate, copper(II) chloride dihydrate, 1,2-diaminobenzene, and phenanthroline hydrate (UkrOrgSyntez Ltd., Ukraine) were used without further purification. Propargylamine and 4-oxocyclohexanecarboxylate were additionally purified by vacuum distillation. Aerosil A-175 was used as a SiO_2 carrier for composite preparation. TEM measurements were performed using a PEM-125 K instrument (SELMI, Ukraine) operating at 100 kV acceleration voltage. Samples were prepared as previously described[48]. Powder X-ray diffraction measurements were performed using Bruker D8 Advance diffractometer with CuKα radiation (λ=1.54056 E). Raman spectra of the composites were measured using MDR-23 spectrometer equipped with an Andor CCD camera and a solid-state laser with an excitation wavelength of λ = 457 nm. Cu content in the composites and the reaction mixtures after experiments was determined by atomic adsorption spectroscopy (AAS) using iCE3500 spectrometer (Thermo Scientific, USA) with acetylene-air flame atomization. Energy-dispersive X-ray spectroscopy (EDX) was carried out on a scanning electron microscope FEI Inspect equipped with EDAX Genesis EDX-System. The values of elements content were averaged for 5 EDX measurements in different places of the sample. The reaction mixtures after the catalytic tests were analyzed by ^{1}H NMR (Bruker Advance 400 spectrometer) using 1,3,5-trimethoxybenzene as an internal standard.

Synthesis of the composites. $Cu(OAc)_2 \cdot H_2O$ or $CuCl_2 \cdot 2H_2O$ and N-containing organic components (DAB or Phen) were fully dissolved in methanol under stirring at 60 ºC (masses of reagents and sample coders are presented in Table S1, Supporting Information). The Cu content in the composites varied from 0.8 to 16.2 %. Then Aerosil powder was added to the solution of copper complex and solvent was evaporated at stirring at 60 ºC until formation of dry powder. The powders were finely grinded, transferred into the ceramic crucibles, and placed in a tubular furnace, which was purged with argon for 15 minutes, then heated to 300-600 ºC depending on pyrolysis temperature (Table 1) at certain heating rate (Table 1), and kept at a set temperature for one hour in an argon atmosphere, then cooled to room temperature in argon.

The catalytic tests were carried out according to a previously published procedure[14]with a 1.5-3 mmol of ethyl 4-oxocyclohexanecarboxylate (1 eq) and propargylamine (2 eq) in isopropyl alcohol at reflux(Scheme 1). After 3.5 h of the reaction the catalyst was separated, the reaction mixture was passed through SiO_2 pad and washed off with chloroform and ethylacetate. The solvents were removed under vacuum and known quantity of 1,3,5-trimethoxybenzene (standard) was added to the residue and dissolved in $CDCl_3$. The reaction mixtures were analized by ^{1}H NMR spectroscopy, the quantities of the compounds were determined by integration of the signals relative to the signals of standard. The yield of the **3** was calculated as ratio of the quantity **3** in the residue after the catalytic test to the initial quantity of the 4-oxocyclohexanecarboxylate (**1**). The weight of the catalysts was

not adjusted to a certain content of Cu or C, because we supposed that both Cu and C could have catalytic activity. To calculate the amount of copper in a sample weight, the copper content determined by the AAS was used.

Results and discussion

The composites Cu@SiO_2-X were obtained by impregnation of Aerosil or activated carbon (Cu@SiO_2-11) with solutions of Cu^{II} complexes (prepared *in situ*) with 1,2-diaminobenzene (DAB) or 1,10-phenanthroline (Phen) followed by pyrolysis of the samples in an argon atmosphere. Two types of starting compounds were taken, i.e., the complexes containing DAB and Phen. Besides, copper and carbon content, temperature of pyrolysis, and pyrolysis rate were varied to reveal the influence of these factors on the performance of the composites in the catalytic reaction.

The content of copper in the composites was analyzed by AAS and EDX methods. According to AAS, overall Cu content in the obtained composites was in the range from 0.8 to 16.2 %. Apparetly, copper particles located on the external surface of the support exhibit catalytic activity, because they are easily accessible to reagent molecules. Therefore, to estimate the amount of copper on the surface of the composite particles, EDX was used as the most suitable method for characterization of the chemical composition of the surface and elemental analysis of insoluble materials. Though this method has some limitations in characterizing samples, it could provide information on the content of C, N, O in the surface layer of the samples. According to EDX data (Table 1), the surface layer contained Cu, C, N, and Si (except Cu@SiO_2-11, which was prepared using activated carbon RWAP-1208 instead of SiO_2). The values of mean mass fractions for Cu were in the range from 2% up to 23%, and these values expectedly grow with the increase of overall Cu content (measured by AAS). This fact may indicate that copper is mainly located on the outer surface of the composite particles and therefore is accessible to reagent molecules.

The mean mass fraction for carbon and nitrogen according to EDX data was in the range of 4% to 56% and 1.6% to 13%, respectively. It is interesting to note that on average the carbon content in the DAB-based composites was higher compared to Phen-based ones, although the carbon content in the DAB was significantly less than in Phen. Probably during pyrolytic destruction, DAB formed more “dense” carbon deposits around copper due to its size smaller than Phen and remained preferably in the composite rather than leaving it in the form of gaseous products.

In the resulting composites, carbon probably forms separate phase, while nitrogen is incorporated into this carboneous phase, resulting in formation of N-doped carbon.

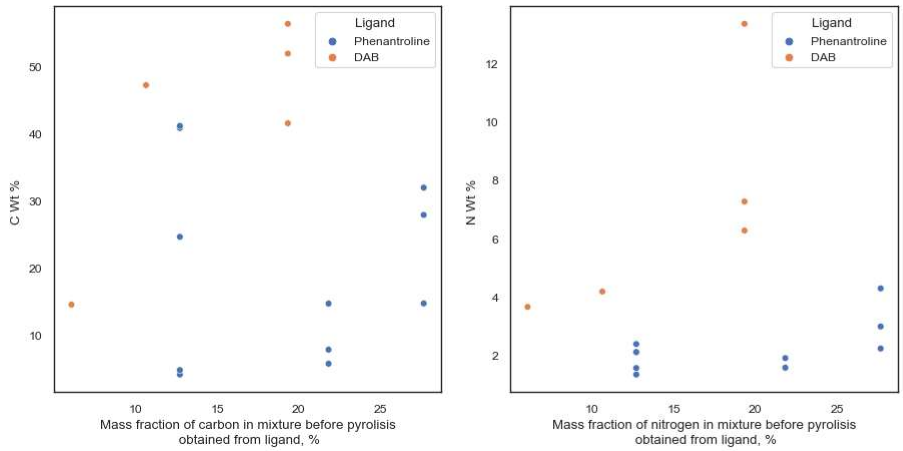

Figure 2. Mass fraction for carbon and nitrogen measured by EDX depending on ligand mass fraction of corresponding element before pyrolysis.

Table 1. Content of elements in the surface layer of the composites measurred by EDX

Sample	Cu, % by weight	C, % by weight	N, % by weight	Si, % by weight	O, % by weight
Cu@SiO_2-3	6.7	27.9	3.0	26.2	36.1
Cu@SiO_2-4	2.0	40.8	2.4	16.6	38.0
Cu@SiO_2-6	9.8	41.6	6.3	14.6	27.6
Cu@SiO_2-9	3.9	51.9	7.3	8.3	28.4
Cu@SiO_2-10	4.2	4.1	1.3	52.8	37.4
Cu@SiO_2-11	9.8	14.6	3.7	36.8	35.1
Cu@SiO_2-12	6.3	14.7	1.6	40.4	36.8
Cu@SiO_2-13	3.7	32.0	4.3	27.1	32.8
Cu@SiO_2-14	4.4	4.8	1.6	51.6	37.5
Cu@SiO_2-15	9.7	7.8	1.9	45.4	34.9
Cu@SiO_2-16	10.3	14.7	2.2	37.7	34.9
Cu@SiO_2-17	3.3	24.6	2.1	30.7	39.2
Cu@SiO_2-18	2.2	47.2	4.2	12.2	34.0
Cu@SiO_2-20	2.0	41.2	2.1	18.7	35.8
Cu@SiO_2-21	7.1	5.7	1.6	50.6	34.8
Cu@C-1	23.1	56.4	13.3	0	6.4

Table 2. Catalyst preparation conditions, identified phases and partciles size calculated from XRD data and yields of **3** for obtained composites

Sample	Cu^{II} salt	Ligand	Ligand: Cu ratio	Cu content [1], %	Temperature of pyrolisis, °C	Pyrolysis rate, °C per minute	Phases identified by XRD	Cu size by Sherrer equation, nm	Yields of **3** [2], %
Cu@SiO_2-2	$Cu(OAc)_2$	Phen	2	0.8	600	5	Cu	26	31
Cu@SiO_2-3	$Cu(OAc)_2$	Phen	2	8.4	300	10	Cu	20	56
Cu@SiO_2-4	$Cu(OAc)_2$	Phen	2	2.9	300	10	Cu	27	51
Cu@SiO_2-5	$CuCl_2$	DAB	0.5	7[4]	400	20	Cu; CuCl	27	48
Cu@SiO_2-6	$Cu(OAc)_2$	DAB	2	16.2	400	4	Cu	28	48
Cu@SiO_2-9	$Cu(OAc)_2$	DAB	2	9.1	400	10	Cu	17[3]	42
Cu@SiO_2-10	$Cu(OAc)_2$	Phen	2	6.6	400	10	Cu	27	33
Cu@SiO_2-11	$CuCl_2$	DAB	0.65	7	600	5	Cu	37	38
Cu@SiO_2-12	$Cu(OAc)_2$	Phen	2	6.4	400	4	Cu; Cu_2O	25	41
Cu@SiO_2-13	$Cu(OAc)_2$	Phen	2	3.3	400	4	Cu	29	27
Cu@SiO_2-14	$Cu(OAc)_2$	Phen	2	3.3	400	4	Cu	31	29
Cu@SiO_2-15	$Cu(OAc)_2$	Phen	2	6,3	400	20	Cu; Cu_2O	30	35
Cu@SiO_2-16	$Cu(OAc)_2$	Phen	2	8.2	400	20	Cu; Cu_2O	27	40
Cu@SiO_2-17	$Cu(OAc)_2$	Phen	2	2.4	400	20	Cu	29	45
Cu@SiO_2-18	$CuCl_2$	DAB	2	4.2	400	20	Cu	33	62
Cu@SiO_2-19	$CuCl_2$	DAB	0.25	11.9	400	20	Cu; CuCl	47[3]	58
Cu@SiO_2-20	$Cu(OAc)_2$	Phen	2	2.9	600	5	Cu	33	28
Cu@SiO_2-21	$Cu(OAc)_2$	Phen	2	7.2	600	5	Cu	31	35
Cu@C-1	$Cu(OAc)_2$	DAB	2	8.8	300	10	Cu	14	46

[1] according to AAS data

[2] after 3.5 hours of the reaction; formula of **3** is shown on Fig. 1

[3] weak XRD signal. Size was calculated for only one peak with $2\theta = 43.3$

[4] value is calculated according to the synthetic procedure

On the powder X-ray diffraction patterns of all samples the peaks at $2\theta = 43.2$ and 50.3 were observed. These peaks correspond to 111 and 200 crystallographic planes of the metallic Cu (Fig. 3) [52,53], thus, metallic Cu was observed in the powder XRD patterns of samples, formed at 300 °C and higher temperatures. It could be concluded that his temperature was already sufficient for the reduction of Cu^{II} by the organic ligands (Phen or DAB).

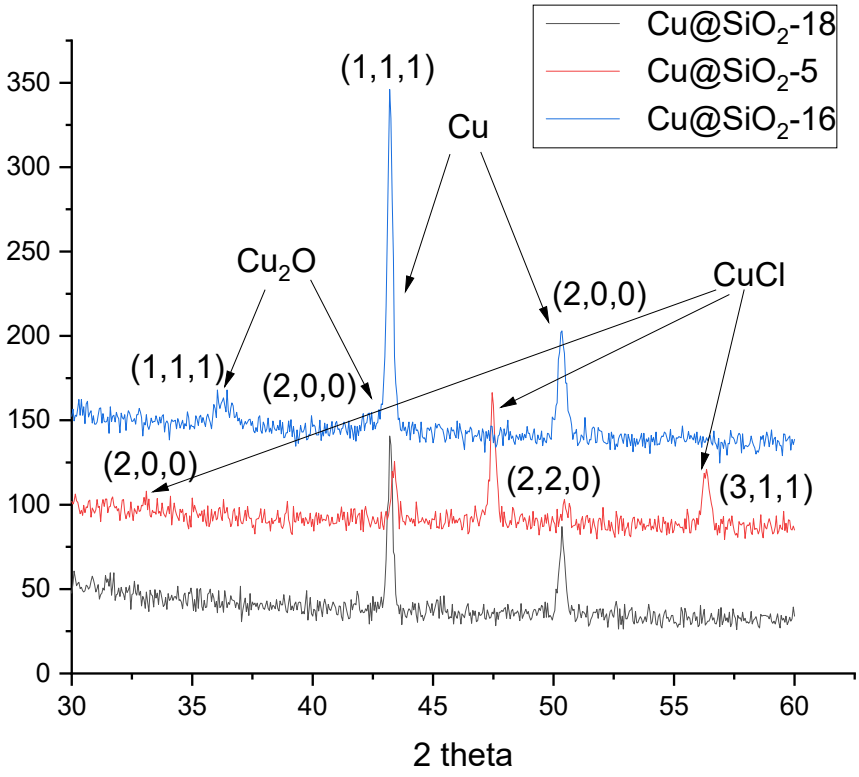

Figure 3. XRD patterns of the representative samples of the composites.

Among the composites prepared from $CuCl_2$, the powder diffraction patterns of the Cu@SiO_2-19 and Cu@SiO_2-5 contained the peaks corresponding to CuCl (2θ = 33.1, 47.4, and 56.3)[54,55]. These composites were obtained at DAB:Cu ratios 0.25 and 0.5, respectively. Formation of CuCl can be explained by an insufficient quantity of the organic ligand for the reduction of Cu^{II} to metallic Cu in these two cases. In the case of Cu@SiO_2-11, DAB:Cu ratio was 0.65 and reflexes of CuCl were not observed on XRD pattern, so the amount of ligand at this level was sufficient for the complete reduction of Cu^{II}. For other composites obtained from $CuCl_2$ no reflections of CuCl were found in the diffraction patterns. The composite Cu@SiO_2-18 was prepared with DAB:Cu ratio equal to 2 and the absence of CuCl in this composite was confirmed by the XRD and EDX methods. Thus, in the case of pyrolysis of samples obtained from the reaction mixtures with ligand:Cu ratio ≥ 0.65, Cu^{II} was completely reduced and chlorine was removed.

In turn, PXRD patterns of Cu@SiO_2-12, Cu@SiO_2-15, and Cu@SiO_2-16 contained the peaks which could be assigned to Cu_2O (2θ = 36.4, 42.3)[56] in addition to the peaks of metallic Cu. These composites were prepared by pyrolysis of complexes obtained from $Cu(Ac)_2$ and Phen with Phen:Cu ratio equal to 2. The same Phen:Cu ratio was used for synthesis of other composites, which did not contain Cu_2O. In contrast to the composites, made from $CuCl_2$, in the case of $Cu(Ac)_2$-Phen system there is apparently no relation between "completeess" of Cu^{II} reduction and ligand-to-copper ratio, because different products formed at the same Phen:Cu ratio.

Thus, pyrolysis of Cu^{II} complexes with DAB and Phen lead to formation of metallic Cu, apparently due to reduction of Cu^{II} with organic ligand or the products of its decomposition. In some cases, the quantity of the organic ligand was, probably, insufficient for complete reduction of all Cu^{II}, and in such cases CuCl or Cu_2O formed (proving this supposition requires detailed studies of the pyrolysis mechanism and evaluation of the balance between Cu^{II} and available reducers, which are different in the cases of Phen and DAB. This task was out of the scope of this study). -Anyhow, the presence of Cu_2O or remaining CuCl did not apparently affect the catalytic activity of the composites.

The size of Cu crystallites in the obtained composites was calculated by Sherrer equation and the values shown in Table 1 are the mean values for sizes, calculated for all reflections (if other is not explicitly stated)[57]. The size of such crystallites according to XRD data varied from 13 nm (Cu@C-1) to 47 nm (Cu@SiO_2-19). We assumed, that the size of Cu particles could be influenced by pyrolisis parameters or composition of mixture. Similarly, copper content in the mixture used for pyrolysis showed no relation to particles size. However, samples obtained at different pyrolysis rates contained particles with very different sizes, so this parameter seems to have no relation to the particles size (Fig. 4a). At the same time, temperature shift from 300 °C to 400 °C and further rise to 600 °C led to bigger particles (Fig. 4b). It also can be noted that composited prepared from DAB complexes generally gave bigger particles.

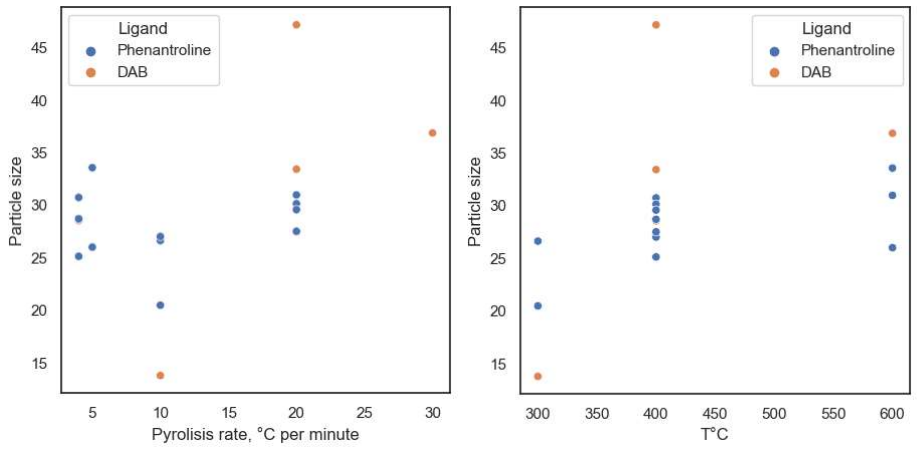

(a) (b)

Figure 4. Mean particles size (determined by Sherrer equation) *vs*. pyrolysis rate (a) and pyrolysis temperature (b).

TEM images of Cu@SiO_2-18 and Cu@SiO_2-19, which provided the highest product yield, are presented in Figure 5. Individual dark spherical particles of about 50 nm size can be observed in TEM images. These particles can be assigned to metallic Cu or core-shell particles Cu@C. The size of particles, found by TEM, exceeds the size of Cu crystallites, estimated by powder XRD (33 and 47 nm, Table 1), the difference can be explained by the presence of a non-crystalline shell on the surface of the particles.

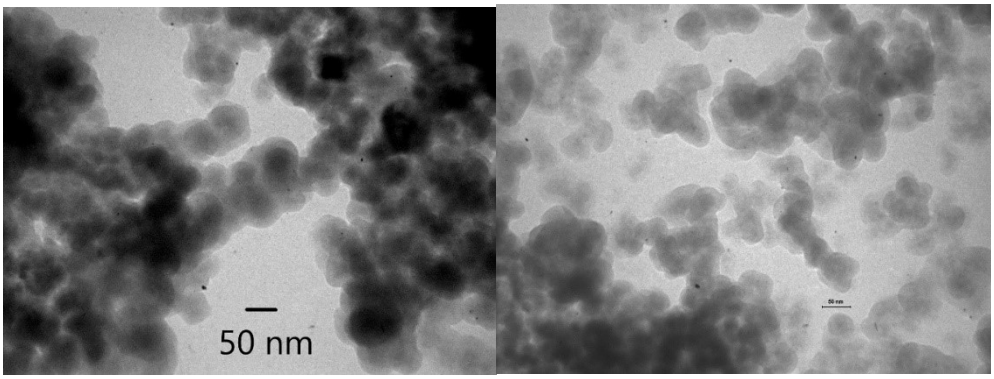

(a) (b)

Figure 5. TEM images of Cu@SiO2-18 (a) and Cu@SiO2-19 (b).

Quite surprisingly, very large Cu partciles were found by SEM in some samples (Fig. 6). Cu particles in the form of polyhedra ranging in size from 150 to 400 nm were found on the SEM image of Cu@SiO_2-4 (Fig. 6(a)) and aggregates of particles of similar size, but elongated shape were found in the case of Cu@SiO_2-9 (Fig. 6(b)).These images were obtained in back-scattered electron mode (BSE) in order to distinguish copper phase phases on the surface unambiguously, because Cu nanoparticles can be observer as the most bright particles due to larger atomic number compared to Si or C. These data do not agree with the results of powder XRD examination, and probably large part of Cu is desposited as smaller particles.

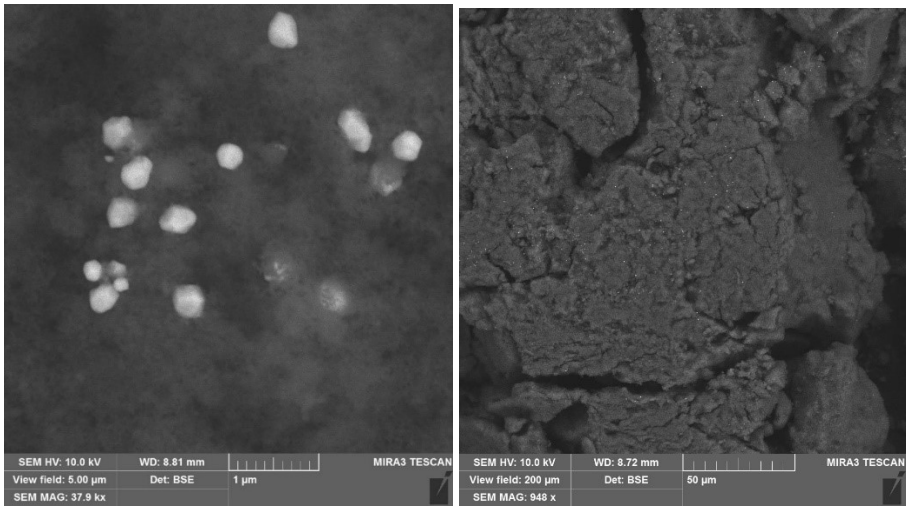

(a)

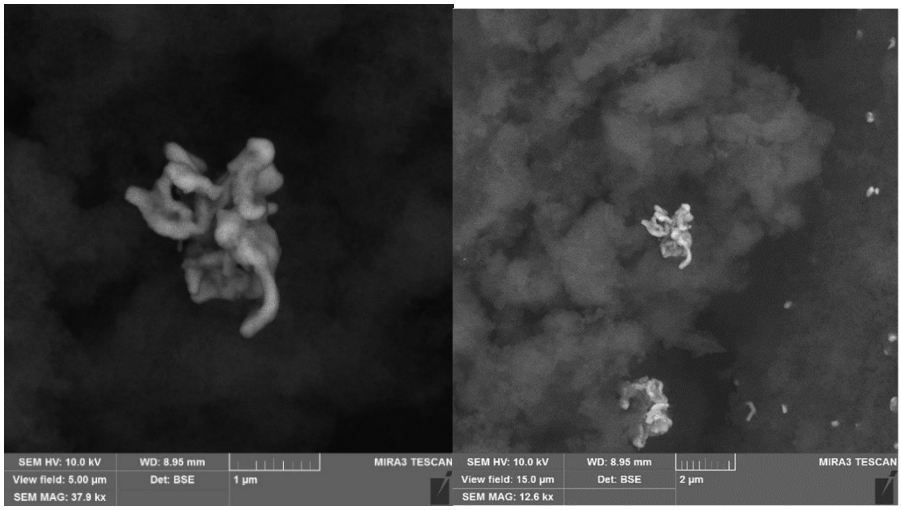

(b)

Figure 6. SEM images of Cu@SiO_2-4 (a) and Cu@SiO_2-9 (b)

In order to obtain information on the carboneous component, Raman spectra of the composites, which provided the highest product yield, were analyzed[58]. Three Raman peaks could be distinguished in the spectra, which were attributed to the bands D (~1350 cm-1), G (~1580 cm-1) and D′(~1620 cm-1), respectively. D-band is characteristic for carbon materials, while D- and D′-bands corresponds to the presence of defects in the graphene structure in such carbon materials[59,60]. The ratio of intensities I(D)/I(G) in case of Cu@SiO_2-18 was 0.8 and in case of Cu@SiO_2-19 it was 1.1, indicating that the latter sample had comparatively more defects in its structure then the former. Analysis of Raman spectra according to [58] allows to assume, that defects in structure of Cu@SiO_2-18 and Cu@SiO_2-19 are the edge defects (Fig. 7).

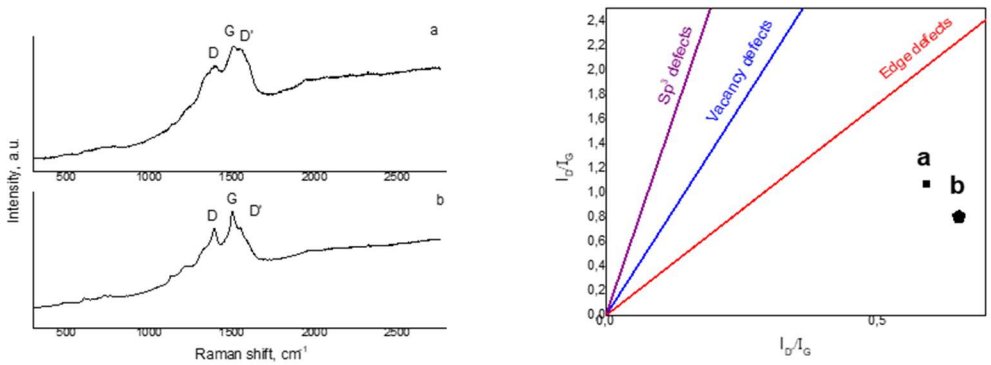

Fig. 7. Raman spectra of Cu@SiO_2-19 (a) and Cu@SiO_2-18 (b) samples and evaluation of type of defects in Cu@SiO_2-19 and Cu@SiO_2-18 (c) (straight lines are drawn according to [58]).

Catalytic properties of the composites

Catalytic tests were carried out according to optimal procedure published in our previous study[14]. As mentioned in the Experimental section, the same weights of the catalysts were used in the experimends (despite different Cu content), because it was supposed that both Cu and C could

have catalytic activity. Use of the same weigths of the composites allowed to plot the yields of the product *vs*. content of different components in the reaction mixtures.

The highest yield of the product **3** was achieved in the case when the reaction mixture contained 4.2 % of Cu, introduced as a composite (Fig. 8). On the other hand, in the reaction mixtures containing more than 5 % of Cu the yield was lower, than in the cases when there was less than 5 % of Cu (hereinafter percents mean mol. % of Cu relative to quantity of **1**). Thus, there was no relation between the the yields of the product and the amount of copper in the reaction mixture. Moreover, the yield in the experimens with Cu-containign composites did not reach the values, previously found for the homogeneous systems containing $CuCl_2$. Such observation can be an evidence that Cu was not completely "washed out" in the experiments; this issue will be considered below in more details.

In separate experimens the quantity of Cu which was "washed out" from the composites to the solution was analyzed. In the case of $Cu@SiO_2$-19, the reaction mixture initially contained 11.9 % of Cu as solid in the composite; after completion of the reaction Cu content in solution was 3.1 % (relative to initial quantity of **1**). In this case, high yield of **3** could be acieved due to dissolved Cu, because addition of 2.5 % of Cu allowed to reach even higher yield (Fig. 8). Situation was completely different for the cases of low Cu loading. Washing out of the same fraction of Cu could not ensure high yield of **3**, if only dissolved Cu was active (Fig. 8). Such analysis gives evidences for the catalytic action of Cu in solid phase, however contribution of the dissolved Cu can't be excluded.

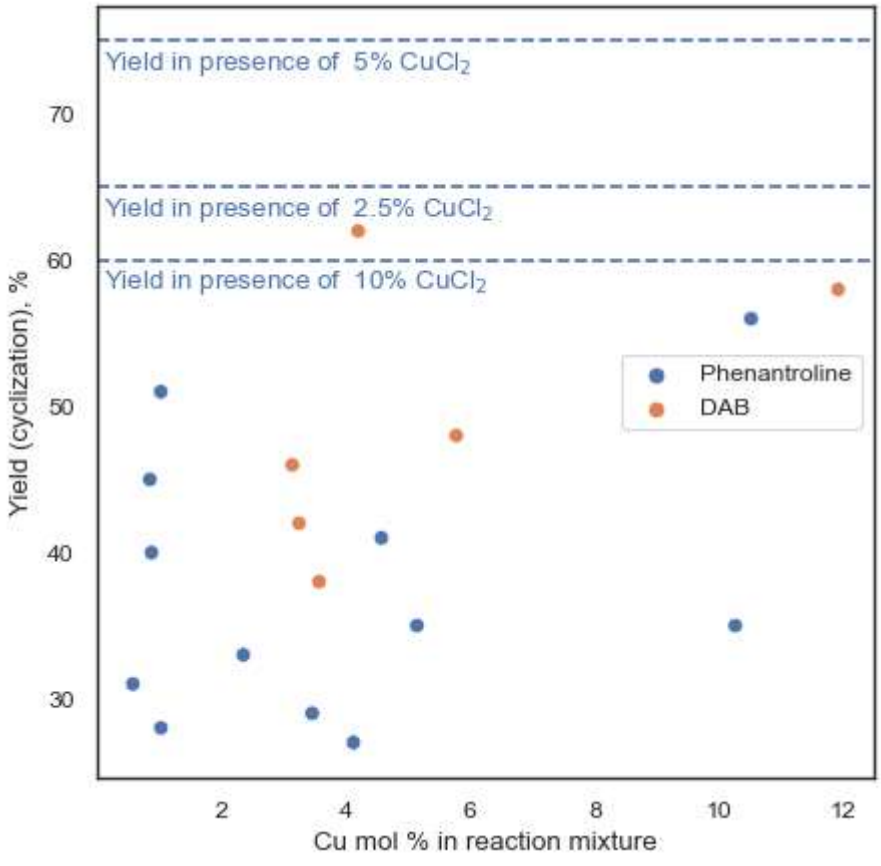

Figure 8. Dependency of product yields on Cu content in the reaction mixture. Solid lines indicate the yields, reached in similar conditions using $CuCl_2$ as soluble catalyst. These lines were plotted using data published in previous article[14].

In order to compare the catalytic properties of different samples, turnover numbers (TON) were calculated as ratio of the 5,6,7,8-tetrahydroquinoline-6-carboxylate quantity (mol) formed after 3.5 h of the reaction to overall copper quantity (mol) in the reaction mixture. Such TON values were in range from 3 to 53, and it can be concluded that Cu content in the reaction mixture did not govern the product yield (or activity of Cu differed in more than 10 times for different composites).

The highest TON values were observed for the cases of composites obtained by pyrolysis of copper complexes with Phen (Fig. 9), while for the reactions, carried out in presence of DAB-based composites high TON values were not observed. In turn, high TON values (>50) were observed for the composites, prepared at different pyrolysis temperatures (Fig. 9(a)), as well as at different pyrolysis rates (Fig. 9(b)), thus there was no correlation between these parameters and catalytic activity.

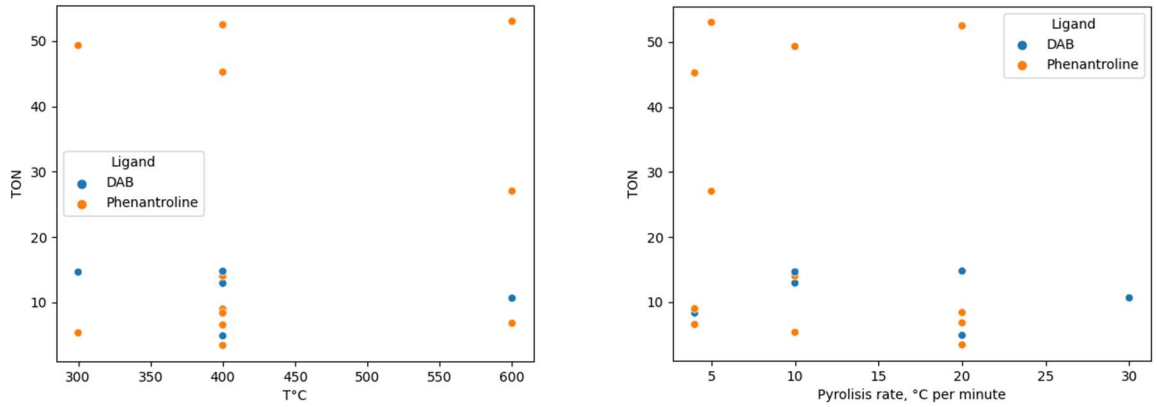

Figure 9. The plots of TON *vs*. pyrolysis temperature (a) and pyrolysis rate (b) applied for synthesis of the composites.

In order to check if the catalytic activity of Cu could be modified by C or N, the plots of TON *vs*. content of carbon and nitrogen in the surface layer of the composites, measured by EDX, were build (Fig. 10). Since identical weights of the composites were used in different experiments, the fractions of C and N in the composites are proportional to their contents in each reaction mixture. No correlation between TON and contents of C, N were found. It just can be noted, that in the case of DAB-based composites higher contents of carbon and nitrogen led to lower TON values, while in the case of Phen-based composites higher TON values were achived.

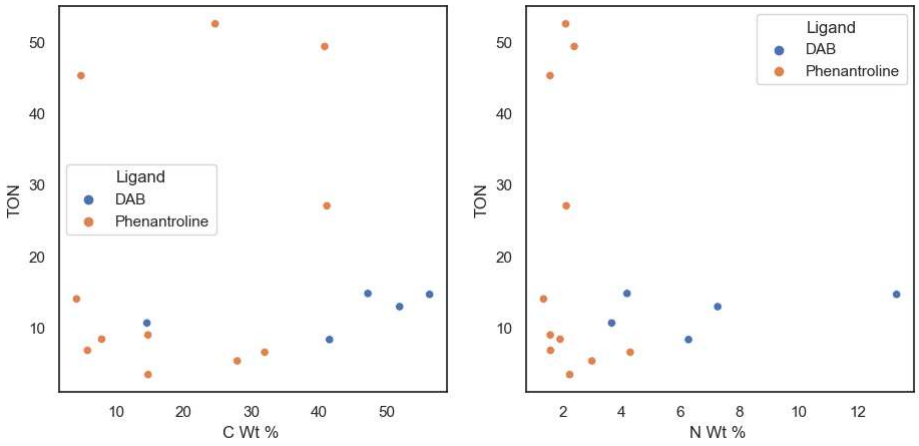

Figure 10. The plots of TON *vs*. content of C and N in the surface layer of the composites, measured by EDX.

According to EDX data, samples Cu@SiO_2-14 and Cu@SiO_2-18, which showed good product yield, had a high carbon content at the 41% and 47% levels. It could be supposed that carbon, along with copper, contributed to the catalytic performance of the composites in this reaction. In order to check this supposition, the yields of **3** were plotted *vs*. parameters X_{Cu} and X_C, which characterized the amounts of copper and carbon, respectively, located on the outer surface of the composites and accessible to the reagent molecules. These parameters X_{Cu} and X_C were calculated as the contents of copper and carbon, respectively, in the composites according to the EDX, multiplied by the mass of the composite in the reaction mixture, taking in mind that the surface of the composites should be similar (the latter supposition is reasonable, because all composites were prepared by decomposition of the complexes on the same support).

On the plot of yields *vs*. X_{Cu} and X_C (Fig. 11), an extended maximum limited by brown area can be observed, this are is approximately located between X_C values 2.75 and 3.75, and for $X_{Cu} < 1.3$. The top of this surface is located at $X_{Cu} = 0.8$ and $X_C = 3.25$. According to the diagram, the yield of product **3** almost does not depend on the X_{Cu} content, because the brown region of the high values of the product yield lies parallel to the 0x axis, but strongly depends on the X_C. This observation can evidence for important role of carbon in catalytic performance of the composites.

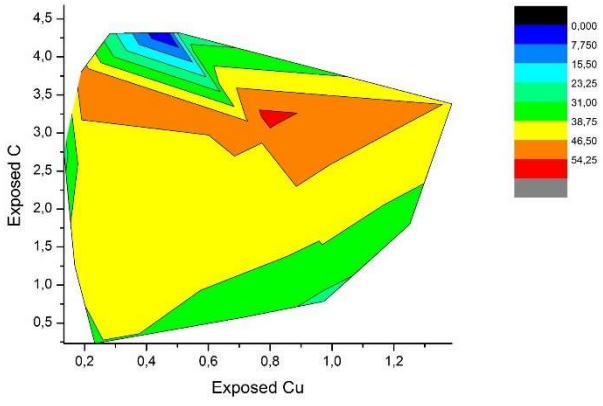

Figure 11. Diagram of yield *vs*. accessible exposed copper and accessible exposed carbon

Reusability and heterogeneity of $Cu@SiO_2$ composites were studied on the example of the $Cu@SiO_2$-18 and $Cu@SiO_2$-19, which were selected as the most productive composites among other samples in this study. According to XRD data, no copper chloride or copper oxide was included in the $Cu@SiO_2$-18. Cu content in this composite was 5.3 % by weight. The first catalytic cycle was carried out with $Cu@SiO_2$-18 during 3.5 h at reflux. The solid residue of $Cu@SiO_2$-18 after the catalytic experiment was separated by filtration, washed with 15 mL isopropyl alcohol, dried under vacuum (15 Torr) at 45 °C and a small amount of the $Cu@SiO_2$-18 and the reaction mixture after the catalytic experiment were analyzed by AAS to determine the copper leaking. The remaining part of $Cu@SiO_2$-18 was used in the next catalytic cycle and copper content in the solid residue of the composite was analyzed again in the same manner. It was found that copper gradually leached out of the $Cu@SiO_2$-18 after each catalytic cycle, and after the 4th cycle, the copper content in the composite decreased to 2.3%. Copper was found by AAS in all reaction mixtures after each catalytic cycle. The yield of the 5,6,7,8-tetrahydroquinoline-6-carboxylate after the second catalytic cycle decreased from 62% to 39% and then it insignificantly decreased in further catalytic cycles, reaching 26% on the fourth cycle. Very similar tendency was found for $Cu@SiO_2$-19.

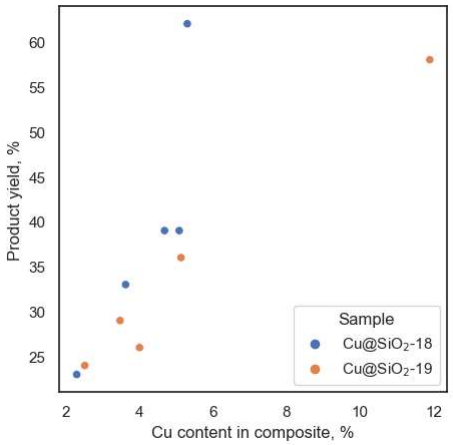

Figure 12. Yield *vs*. copper content on same sample in the series of consequent experiments

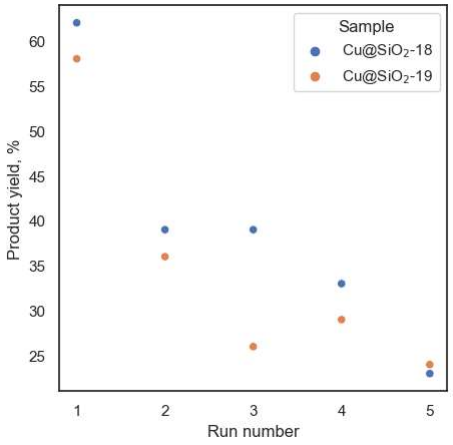

Figure 13. Decreasing yield of 3 in the series of consequent experiments

It should be noted, that for the series of samples, obtained by consequent "washing out" of copper from the same statring material, the yield of the product **3** linearly depended on Cu content in the reaction mixture, implying that all Cu atoms in the composite have similar specific catalytic activity.

Conclusions

In the study a series of Cu-containing composites was prepared by thermal decomposition of Cu^{II} complexes with Phen and DAB deposited on Aerosil. One sample (Cu@C-1) uses activated carrbon RWAP-1208 instead of silica powder. The obtained composites contained metallic copper as nanoparticles along with significant quantity of N-doped carbon, which formed upon pyrolysis of the organic ligands. It was shown in the catalytic experimends, that the composites catalyzed reaction of propargylamine with ethyl 4-oxocyclohexanecarboxylate leading to ethyl 5,6,7,8-tetrahydroquinoline-6-carboxylate. Such catalytic activity originated from the active sites on the surface of the composite, however contribution of the dissolved Cu cannot be excluded. It was found that Cu content in the reaction mixture was not the factor, which controlled the yield of the product. Quite unexpectedly, both content of Cu and C were responsible for formation of the product, and the product yield was more sensitive to the value of carbon surface, exposed to the reagents, rather than to the value of exposed copper surface.

The composites developed in can be directly used in flow reactors for synthesis of fused pyridines, however their stability is still insufficient and should be improved. However, an important finding is that the carbon plays important role in reaction of ketones with propargylamine. This finding can give rise to new research directed on development of active catalysts for the considered reaction. In addition, this work is a one more step towards development of noble-metal-free catalysts for organic reactions, in particular, for replacement of Au-based catalysts of cycloaddition of propargylamine to ketones.

References

[1] O. O. Grygorenko, D. M. Volochnyuk, S. V. Ryabukhin, D. B. Judd, *Chem. - A Eur. J.* **2020**, *26*, 1196–1237.

[2] M. D. Shultz, *J. Med. Chem.* **2019**, *62*, 1701–1714.

[3] G. Seibert, M. Limbert, I. Winkler, T. Dick, *Infection* **1983**, *11*, 275–279.

[4] D. S. Huang, E. V. Leblanc, T. Shekhar-Guturja, N. Robbins, D. J. Krysan, J. Pizarro, L. Whitesell, L. E. Cowen, L. E. Brown, *J. Med. Chem.* **2020**, *63*, 2139–2180.

[5] B. E. Blass, R. Gao, K. M. Blattner, J. C. Gordon, D. A. Pippin, D. J. Canney, *Med. Chem.*

Res. **2022**, *31*, 337–349.

[6] Z. Zhang, Z. Guo, X. Xu, D. Cao, H. Yang, Y. Li, Q. Shi, Z. Du, X. Guo, X. Wang, D. Chen, Y. Zhang, L. Chen, K. Zhou, J. Li, M. Geng, X. Huang, B. Xiong, *J. Med. Chem.* **2021**, *64*, 16650–16674.

[7] L. Wortmann, B. Lindenthal, P. Muhn, A. Walter, R. Nubbemeyer, D. Heldmann, L. Sobek, F. Morandi, A. K. Schrey, D. Moosmayer, J. Günther, J. Kuhnke, M. Koppitz, U. Lücking, U. Röhn, M. Schäfer, K. Nowak-Reppel, R. Kühne, H. Weinmann, G. Langer, *J. Med. Chem.* **2019**, *62*, 10321–10341.

[8] Y. A. Tahirovic, V. M. Truax, R. J. Wilson, E. Jecs, H. H. Nguyen, E. J. Miller, M. B. Kim, K. M. Kuo, T. Wang, C. S. Sum, M. E. Cvijic, G. M. Schroeder, L. J. Wilson, D. C. Liotta, *ACS Med. Chem. Lett.* **2018**, *9*, 446–451.

[9] E. Jecs, Y. A. Tahirovic, R. J. Wilson, E. J. Miller, M. Kim, V. Truax, H. H. Nguyen, N. S. Akins, M. Saindane, T. Wang, C. S. Sum, M. E. Cvijic, G. M. Schroeder, S. L. Burton, C. A. Derdeyn, L. Xu, Y. Jiang, L. J. Wilson, D. C. Liotta, *J. Med. Chem.* **2022**, *65*, 4058–4084.

[10] H. H. Nguyen, Y. A. Tahirovic, V. M. Truax, R. J. Wilson, E. Jecs, E. J. Miller, M. B. Kim, N. S. Akins, L. Xu, Y. Jiang, T. Wang, C. S. Sum, M. E. Cvijic, G. M. Schroeder, L. J. Wilson, D. C. Liotta, *ACS Med. Chem. Lett.* **2021**, *12*, 1605–1612.

[11] E. Vitaku, D. T. Smith, J. T. Njardarson, *J. Med. Chem.* **2014**, *57*, 10257–10274.

[12] G. Abbiati, A. Arcadi, G. Bianchi, S. Di Giuseppe, F. Marinelli, E. Rossi, *J. Org. Chem.* **2003**, *68*, 6959–6966.

[13] L. Abahmane, A. Knauer, U. Ritter, J. M. Köhler, G. A. Groß, *Chem. Eng. Technol.* **2009**, *32*, 1799–1805.

[14] S. O. Sotnik, A. I. Subota, A. Y. Kliuchynskyi, D. V. Yehorov, A. S. Lytvynenko, A. B. Rozhenko, S. V. Kolotilov, S. V. Ryabukhin, D. M. Volochnyuk, *J. Org. Chem.* **2021**, *86*, 7315–7325.

[15] K. Liu, Y. Wang, P. Cheng, Y. Liu, C. Kong, Z. Yi, M. Li, Q. Liu, W. Zhong, H. Takagi, D. Wang, *Ind. Crops Prod.* **2018**, *119*, 226–236.

[16] H. Mao, Y. Shen, Q. Zhang, M. Ulaganathan, S. Zhao, Y. Yang, H. H. Hng, *Carbon N. Y.* **2016**, *96*, 75–82.

[17] B. Cornils, W. A. Herrmann, I. T. Horváth, W. Leitner, S. Mecking, H. Olivier-Bourbigou, D. Vogt, Eds. , *Multiphase Homogeneous Catalysis*, Wiley, **2005**.

[18] S. V. Kolotilov, A. S. Lytvynenko, S. A. Sotnik, *Curr. Inorg. Chem.* **2018**, *7*, 89–105.

[19] A. S. Lytvynenko, S. V. Kolotilov, M. A. Kiskin, O. Cador, S. Golhen, G. G. Aleksandrov, A. M. Mishura, V. E. Titov, L. Ouahab, I. L. Eremenko, V. M. Novotortsev, *Inorg. Chem.* **2014**, *53*, 4970–4979.

[20] A. S. Lytvynenko, R. A. Polunin, M. A. Kiskin, A. M. Mishura, V. E. Titov, S. V. Kolotilov,

V. M. Novotortsev, I. L. Eremenko, *Theor. Exp. Chem.* **2015**, *51*, 54–61.

[21] C. Gao, F. Lyu, Y. Yin, *Chem. Rev.* **2021**, *121*, 834–881.

[22] M. B. Gawande, A. Goswami, F.-X. Felpin, T. Asefa, X. Huang, R. Silva, X. Zou, R. Zboril, R. S. Varma, *Chem. Rev.* **2016**, *116*, 3722–3811.

[23] M. Sankar, Q. He, R. V. Engel, M. A. Sainna, A. J. Logsdail, A. Roldan, D. J. Willock, N. Agarwal, C. J. Kiely, G. J. Hutchings, *Chem. Rev.* **2020**, *120*, 3890–3938.

[24] S. A. Sotnik, K. S. Gavrilenko, A. S. Lytvynenko, S. V. Kolotilov, *Inorganica Chim. Acta* **2015**, *426*, 119–125.

[25] S. S.-Y. Chui, S. M.-F. Lo, J. P. H. Charmant, A. G. Orpen, I. D. Williams, *Science (80-.).* **1999**, *283*, 1148–1150.

[26] D. Sharma, S. Rasaily, S. Pradhan, K. Baruah, S. Tamang, A. Pariyar, *Inorg. Chem.* **2021**, *60*, 7794–7802.

[27] C. S. Budi, D. Saikia, C. S. Chen, H. M. Kao, *J. Catal.* **2019**, *370*, 274–288.

[28] J. Yang, Y. He, J. He, Y. Liu, H. Geng, S. Chen, L. Lin, M. Liu, T. Chen, Q. Jiang, B. M. Weckhuysen, W. Luo, Z. Wu, *ACS Catal.* **2022**, *12*, 1847–1856.

[29] Z. Dong, H. Pan, L. Yang, L. Fan, Y. Xiao, J. Chen, W. Wang, *J. Saudi Chem. Soc.* **2022**, *26*, 101397.

[30] X. Liu, X. S. Luo, H. L. Deng, W. Fan, S. Wang, C. Yang, X. Y. Sun, S. L. Chen, M. H. Huang, *Chem. Mater.* **2019**, *31*, 5421–5430.

[31] S. Y. Ding, J. Gao, Q. Wang, Y. Zhang, W. G. Song, C. Y. Su, W. Wang, *J. Am. Chem. Soc.* **2011**, *133*, 19816–19822.

[32] Y. Han, M. Zhang, Y. Q. Zhang, Z. H. Zhang, *Green Chem.* **2018**, *20*, 4891–4900.

[33] V. P. Petranovskii, A. N. Pestryakov, L. K. Kazantseva, C. B, F. F. Arraza, M. H. Farías, *Int. J. Mod. Phys. B* **2005**, *19*, 2333–2338.

[34] P. Krawiec, E. Kockrick, P. Simon, G. Auffermann, S. Kaskel, *Chem. Mater.* **2006**, *18*, 2663–2669.

[35] R. J. White, R. Luque, V. L. Budarin, J. H. Clark, D. J. Macquarrie, *Chem. Soc. Rev.* **2009**, *38*, 481–494.

[36] V. S. Garcia-Cuello, L. Giraldo, J. C. Moreno-Piraján, *J. Chem. Eng. Data* **2011**, *56*, 1167–1173.

[37] R. Guo, X. Zhang, Z.-N. Hu, D. Niu, X. Li, H. Sun, Q. Liang, *J. Environ. Chem. Eng.* **2023**, *11*, 109143.

[38] C. R. Tubío, J. Azuaje, L. Escalante, A. Coelho, F. Guitián, E. Sotelo, A. Gil, *J. Catal.* **2016**, *334*, 110–115.

[39] R. Lebl, Y. Zhu, D. Ng, C. H. Hornung, D. Cantillo, C. O. Kappe, *Catal. Today* **2022**, *383*, 55–63.

[40] Y. Guo, Y. Gao, X. Li, G. Zhuang, K. Wang, Y. Zheng, D. Sun, J. Huang, Q. Li, *Chem. Eng. J.* **2019**, *362*, 41–52.

[41] Y. Chen, T. Zhang, Q. Liu, *Int. J. Hydrogen Energy* **2021**, *46*, 30373–30381.

[42] J. R. Deka, D. Saikia, P.-H. Chen, K.-T. Chen, H.-M. Kao, Y.-C. Yang, *J. Ind. Eng. Chem.* **2021**, *104*, 529–543.

[43] K. Murugesan, A. M. Alenad, A. S. Alshammari, M. Sohail, R. V. Jagadeesh, *Tetrahedron* **2021**, *102*, 132526.

[44] Ö. Karahan, E. Biçer, A. Taşdemir, A. Yürüm, S. A. Gürsel, *Eur. J. Inorg. Chem.* **2018**, *2018*, 1073–1079.

[45] F. Chen, A.-E. Surkus, L. He, M.-M. Pohl, J. Radnik, C. Topf, K. Junge, M. Beller, *J. Am. Chem. Soc.* **2015**, *137*, 11718–11724.

[46] F. A. Westerhaus, R. V. Jagadeesh, G. Wienhöfer, M.-M. Pohl, J. Radnik, A.-E. Surkus, J. Rabeah, K. Junge, H. Junge, M. Nielsen, A. Brückner, M. Beller, *Nat. Chem.* **2013**, *5*, 537–543.

[47] V. M. Asaula, O. V. Shvets, O. O. Pariiska, V. V. Bur'yanov, S. V. Ryabukhin, D. M. Volochnyuk, S. V. Kolotilov, *Theor. Exp. Chem.* **2020**, *56*, 261–267.

[48] V. M. Asaula, V. V. Buryanov, B. Y. Solod, D. M. Tryus, O. O. Pariiska, I. E. Kotenko, Y. M. Volovenko, D. M. Volochnyuk, S. V. Ryabukhin, S. V. Kolotilov, *European J. Org. Chem.* **2021**, *2021*, 6616–6625.

[49] R. V. Jagadeesh, H. Junge, M.-M. Pohl, J. Radnik, A. Brückner, M. Beller, *J. Am. Chem. Soc.* **2013**, *135*, 10776–10782.

[50] X. Liu, L. Dai, *Nat. Rev. Mater.* **2016**, *1*, 16064.

[51] A. A. Abakumov, I. B. Bychko, O. V. Selyshchev, D. R. T. Zahn, X. Qi, J. Tang, P. E. Strizhak, *Carbon N. Y.* **2020**, *157*, 277–285.

[52] T. Theivasanthi, M. Alagar, **2010**.

[53] E. A. Owen, E. L. Yates, *London, Edinburgh, Dublin Philos. Mag. J. Sci.* **1933**, *15*, 472–488.

[54] S. Liu, H. Hou, W. Hu, X. Liu, J. Duan, R. Meng, *RSC Adv.* **2016**, *6*, 3742–3747.

[55] J. Zemann, *Acta Crystallogr.* **1965**, *18*, 85–237.

[56] J. He, Y. Jiang, J. Peng, C. Li, B. Yan, X. Wang, *J. Mater. Sci.* **2016**, *51*, 9696–9704.

[57] A. L. Patterson, *Phys. Rev.* **1939**, *56*, 978–982.

[58] A. Eckmann, A. Felten, A. Mishchenko, L. Britnell, R. Krupke, K. S. Novoselov, C. Casiraghi, *Nano Lett.* **2012**, *12*, 3925–3930.

[59] O. Y. Posudievsky, A. S. Kondratyuk, O. A. Kozarenko, V. V. Cherepanov, V. L. Karbivskiy, V. G. Koshechko, V. D. Pokhodenko, *Electrochim. Acta* **2021**, *399*, 139410.

[60] O. Y. Posudievsky, A. S. Kondratyuk, O. A. Kozarenko, V. V. Cherepanov, G. I. Dovbeshko, V. G. Koshechko, V. D. Pokhodenko, *Carbon N. Y.* **2019**, *152*, 274–283.